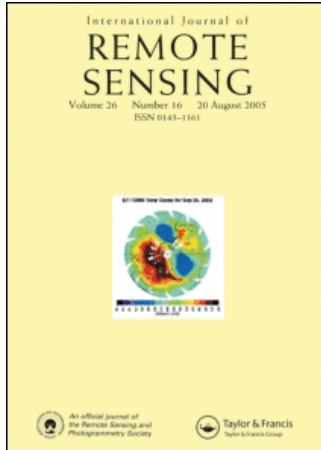


This article was downloaded by:[UT Arlington]
On: 7 September 2007
Access Details: [subscription number 768486108]
Publisher: Taylor & Francis
Informa Ltd Registered in England and Wales Registered Number: 1072954
Registered office: Mortimer House, 37-41 Mortimer Street, London W1T 3JH, UK



International Journal of Remote Sensing

Publication details, including instructions for authors and subscription information:
<http://www.informaworld.com/smpp/title~content=t713722504>

A satellite view of internal waves induced by the Indian Ocean tsunami

Online Publication Date: 01 July 2007

To cite this Article: Santek, D. A. and Winguth, A. (2007) 'A satellite view of internal waves induced by the Indian Ocean tsunami', International Journal of Remote Sensing, 28:13, 2927 - 2936

To link to this article: DOI: 10.1080/01431160601094534

URL: <http://dx.doi.org/10.1080/01431160601094534>

PLEASE SCROLL DOWN FOR ARTICLE

Full terms and conditions of use: <http://www.informaworld.com/terms-and-conditions-of-access.pdf>

This article maybe used for research, teaching and private study purposes. Any substantial or systematic reproduction, re-distribution, re-selling, loan or sub-licensing, systematic supply or distribution in any form to anyone is expressly forbidden.

The publisher does not give any warranty express or implied or make any representation that the contents will be complete or accurate or up to date. The accuracy of any instructions, formulae and drug doses should be independently verified with primary sources. The publisher shall not be liable for any loss, actions, claims, proceedings, demand or costs or damages whatsoever or howsoever caused arising directly or indirectly in connection with or arising out of the use of this material.

© Taylor and Francis 2007

A satellite view of internal waves induced by the Indian Ocean tsunami

D. A. SANTEK*† and A. WINGUTH‡

†Cooperative Institute for Meteorological Satellite Studies, University of Wisconsin-Madison, 1225 West Dayton Street, Madison, WI 53706, USA

‡Department of Atmospheric and Oceanic Sciences, University of Wisconsin-Madison, 1225 West Dayton Street, Madison, WI 53706, USA

At 08:45 local time (02:45 GMT) on 26 December 2004, 1 h and 45 min after the Sumatra Earthquakes of magnitude 9.3, a devastating tsunami struck the east coast of Sri Lanka. Nearly 2 h and 30 min after the wave hit the coast, a weather satellite passed over Sri Lanka's coastal zone providing a rare glimpse of internal waves along the continental slope due to this tsunami. The satellite imagery indicates wave-like features from the tsunami being reflected, diffracted, and scattered off the steep continental slope and submarine canyons adjacent to Sri Lanka. The energetic wave and its modification to internal waves possibly eroded sediment from the sea floor and transported it to the sea surface. Solitary features generated by internal waves can explain the observed pattern. Future modelling approaches considering these nonlinear interactions would be required for a better understanding of the tsunami behaviour in the coastal zone, where its destructive effects are most prominent.

1. Introduction

The east coast of Sri Lanka comprises the south-eastern part of the Bay of Bengal, located in the north-eastern part of the Indian Ocean. The water depth in the Bay of Bengal varies between 10 m in the shelf area of Bangladesh to more than 4500 m at the Equator with by far the largest deep-sea fan of the Earth. Its sedimentary infill is largely terrigenous material derived from the Himalayas and transported through the Ganges–Brahmaputra Rivers into the northern Indian Ocean. The continental slope near the east coast of Sri Lanka is one of the world's steepest bathymetric features with several submarine canyons exceeding 45° in some locations. The geology of the shelf near Batticaloa at the coast of Sri Lanka encompasses coral reefs and sandy clay over gravel (International Indian Ocean Expedition 1964). The stratified water masses of the Sri Lanka east coast represent the low-salinity portion of the northern Indian Ocean caused by the high seasonally varying river runoff and precipitation contrary to the high-salinity waters of the Arabian Sea. In the Bay of Bengal, part of the northern Indian Ocean, the circulation is characterized by a strong seasonal variability. During the north-east monsoon in December, a cyclonic (anti-clockwise) flow and a strong southward-directed East Indian Coastal Current is observed from ship drift data (Cutler and Swallow 1984) and from Topex/Poseidon altimeter data (Eigenheer and Quadfasel 1999). This low-salinity (<34) current spreads westward into the Arabian Sea and can exceed 1.8 m s^{-1} (Wyrтки 1973). Superimposed on this circulation are planetary mode waves and interannual

*Corresponding author. Email: dave.santek@ssec.wisc.edu

variations related to the El Niño Southern Oscillation (Srinivas *et al.* 2005), which influences the concentration of nutrients and hence organic matter at the sea surface (Kumar and Ramesh 2005). With lower nutrient concentrations offshore, pigment concentrations of phytoplankton decrease from the shelf region of Sri Lanka in the offshore direction.

Tsunamis are assumed to be long-period surface gravity waves triggered by coastal earthquakes, landslides, or volcanoes that obey, with their high energy, the generalized equations of phase speed c_s and group speed c_g for waves (LeBlond and Mysak 1978)

$$c_s = \sqrt{\frac{g}{k} \tanh(kH)} \quad (1)$$

$$c_g = \frac{c_s}{2} \left[1 + \frac{2kH}{\sinh 2kH} \right]. \quad (2)$$

For tsunamis, equations (1) and (2) can be approximated with $kH \ll 1$ to $c_s = \sqrt{gH}$ and $c_s = c_g$, where k is the wavenumber, g the acceleration due to gravity, and H the depth of the water. In this assumption, the wave speed is non-dispersive (does not depend on the wavelength), and a single frequency applies. Thus, the speed of the wave can be estimated if the depth of the ocean sea floor is known. The tsunami travelled in the Indian Ocean where the depth is about 4000 m, giving it a phase speed of about 200 m s^{-1} . An initial wavelength of $\sim 500 \text{ km}$ and change in sea level of about 70 cm have been detected from the Jason 1 altimeter satellite (Gower 2005). When the wave approached the continental slope of Sri Lanka, parts of it were transmitted, reflected, and scattered and possibly generated internal waves. The tsunami likely generated suspended sediment (Pennish 2005) on the upslope and shallow water (McCave 2003), and transported finer sediment compositions to near the surface.

Internal solitary waves are generated by nonlinear deformation of long waves like internal tides or tsunamis. They are a widespread and prominent feature in the oceans (Osborne and Burch 1980), and lakes (Farmer 1978) and are commonly associated with density stratification. For example, satellite images off Gibraltar (Da Silva *et al.* 1998) reveal their distribution and propagation by an alteration of the sea-surface roughness formed by a surface-internal wave current interaction of some type, sometimes modified by suspended matter, but the generation mechanisms are still controversially discussed (e.g. Nittrouer and Wright 1994, Farmer and Armi 1999, Small 2001a, b, Cacchione *et al.* 2002). Internal solitary waves occur particularly near regions of variable bathymetry, such as shelf edges, seamounts, sills, and submarine canyons, where the bathymetry forces the pycnocline to oscillate with the frequency of the tidal wave or tsunami. Such conditions apply to the coast of Sri Lanka (Quadfasel 1998).

In this paper, we analyse remote-sensing features in the region of Batticaloa on the eastern coast of Sri Lanka where the tsunami, with wave heights of 4–7 m, caused several thousand fatalities and injuries (Liu *et al.* 2005).

2. Data and methodology

The National Aeronautics and Space Administration's (NASA) research satellite, Terra, a polar orbiting satellite carrying the Moderate Resolution Imaging

Spectroradiometer (MODIS) instrument, passed over Sri Lanka on the morning of 26 December 2004. The MODIS instrument is a 36-channel imager consisting of visible/near-infrared (VNIR) channels at 250-m and 500-m resolution, and thermal infrared (TIR) at 1-km resolution at nadir. The instrument is designed for multi-discipline research, with sensors in spectral bands for atmosphere, ocean, and land interests. The spectral range in the VNIR wavelengths is 0.4–2.1 μm , and in the TIR 3.6–14.3 μm (Barnes *et al.* 1998). The data, in Level 1B format, were retrieved from the Goddard Earth Sciences Distributed Active Archive Center. The Level 1B format provides geolocated and calibrated radiances in the original satellite perspective. The calibration procedure to convert sensor-output digital numbers to reflected radiance for the VNIR bands and thermally emitted radiance for the TIR bands is described in Guenther *et al.* (1998). An inverse Planck function is used to convert TIR emitted radiances to brightness temperatures (Petty 2004).

Figure 1 depicts a true-colour MODIS image of this pass by colour-combining spectral band 1 (620–670 nm), band 4 (545–565 nm), and band 3 (459–479 nm), corresponding to red, green, and blue wavelengths. The MODIS instrument is capable of detecting significant disturbances in the sea by changes in the reflectivity of the water column (figure 2).

3. Results and discussion

The left panel of figure 2 shows the reflectivity in the coastal zone before the perturbation of the tsunami (19 December 2004, 05:10 GMT). High reflectance on the shelf is likely associated with suspended sediment by wind-induced wave-disturbances. The reflectivity is also affected by biological activity such as phytoplankton and zooplankton (Curran and Novo 1988), and subsurface plankton blooms have been identified during past surveys of the shelf (e.g. during the International Indian Ocean Expedition 1964). In contrast to the relatively undisturbed case, the right panel shows the situation for 26 December 2004, 05:15 GMT or about 2 h and 30 minutes after the tsunami hit the shore of the east coast of Sri Lanka. Additional remote-sensing data for other times were influenced by strong cloud coverage because of Sri Lanka's close proximity to the Intertropical Convergence Zone (ITCZ).

The features in figure 2 are likely generated by an internal wave due to the tsunami which itself was reflected, diffracted, and scattered off the continental slope. Two types of waves can be seen in figure 2: linear and bow waves. These wave patterns match well the strong bathymetric gradient. The linear wave features are likely generated by reflection, near the straight continental slope, while bow waves can be created on canyons or sea mounts.

Figure 3 shows the high-gradient bathymetry region overlaid on the wave image. This region is 25 km wide where the ocean depth decreases from 3000 m to 50 m, moving from east to west. The reflected waves emanate from the left side of the high-gradient region, which is the shelf break. Several submarine canyons adjacent to the shelf off the coast of Sri Lanka had been identified during the International Indian Ocean Expedition and measured to depths of 1000–1500 m. Interestingly, the measured wavelength between the peaks of high reflectivity is about 6 km, which would be far too short for the period (~ 40 min) and shallow-water equation (1). According to analytic theories of tsunamis, the wave characteristics change substantially if they are scattered and reflected by a bathymetric feature like a steep continental slope, submarine canyons, or seamount (Mofjeld *et al.* 2000).

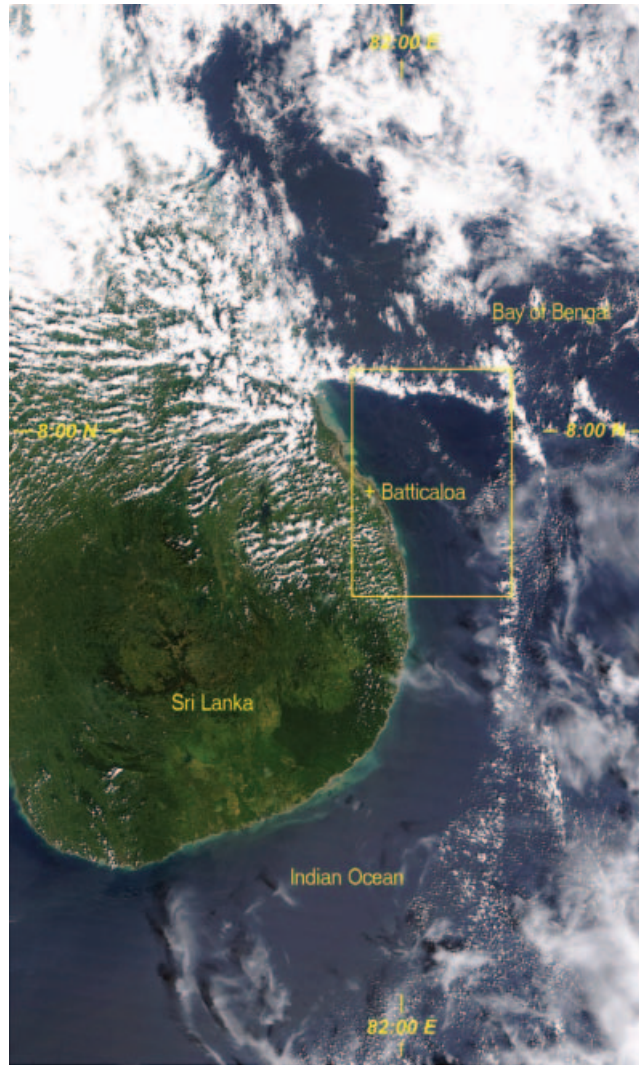


Figure 1. True-colour image from MODIS over the eastern half of Sri Lanka and adjacent Indian Ocean. This is from 05:10 GMT on 26 December 2004. The yellow box is a cloud-free region near Batticaloa where we looked for oceanic evidence of the tsunami. (Courtesy of Liam Gumley, Space Science and Engineering Center, University of Wisconsin-Madison.)

Internal waves at surfaces between different density layers can be created by a tsunami pushing on the continental slope. The currents resulting from the internal waves interact with wind-generated surface waves to produce alternate bands of rough and calm water that are visible from space (Garret 2003). For long internal waves, the phase wave speed (equation(1)) modifies to $c_s = \sqrt{g'h_1}$ with reduced gravity $g' = g\Delta\rho/\rho_1$, density difference between the two density layers $\Delta\rho$, and density of the upper layer ρ_1 . For $\Delta\rho = 5 \text{ kg m}^{-3}$, $\rho_1 = 1021 \text{ kg m}^{-3}$ (see BENGALWOCE, Quadfasel 1998), and $h_1 = 150 \text{ m}$ for the surface layer, the computed wavelength of the internal wave (6.4 km) is close to the 6-km wavelength shown on the MODIS image in figure 2. Over bathymetric features, internal waves may change currents, create a collapse of the mixed layer, and generate solitary wave patterns (Farmer

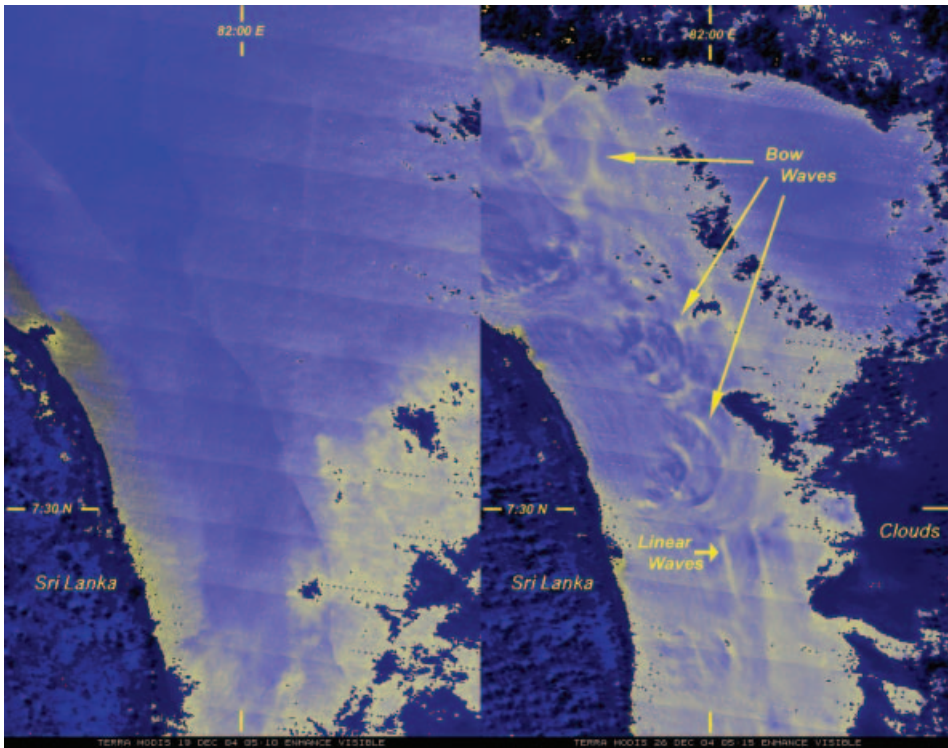


Figure 2. Enhanced, colour image taken off the eastern coast of Sri Lanka, using two visible channels (band 1 and 2) from the MODIS instrument from 1 week earlier (on the left) and less than 2.5 h after the tsunami hit on the right. The range of reflected radiance over the ocean is about $6 \text{ W m}^{-2} \text{ sr}^{-1} \mu\text{m}^{-1}$. The solar zenith angle is 36° for both days. The distance from shore to the bow wave in the middle is about 16 km. The distance between waves is about 6 km.

and Armi 1999). Low-frequency internal waves are reflected off the sloping bottom toward the open ocean, while internal waves with frequencies $\omega > [(f^2 + N^2 \alpha^2) / (1 + \alpha^2)]^{1/2}$ are deflected towards the head of canyons (Hotchkiss and Wunsch 1982). f is the Coriolis parameter, N the buoyancy frequency, and α the slope of the canyon bottom axis. The energy of these reflected waves points approximately in the direction of the local gravity vector (LeBlond and Mysak 1978, Cacchione *et al.* 2002). Curvature of the wavefront, as seen in the MODIS images, is potentially related to refractions of rays by variations in the water depth, nonlinear wave interactions, and stratifications (Small 2001a, b). Shallowing of the wave affects refraction because the phase speed of a nonlinear internal wave depends on its amplitude. The internal waves interact with short wind-driven waves generating patterns similar to images from the MODIS instrument (figures 1–3).

Takayama and Saito (2004) proposed that tsunamis with their high speed in the deep ocean may be treated as quasi-supersonic waves. Patterns of such a shock wave and Mach reflection of shallow water waves (Toro *et al.* 1999) are significantly different from those of a traditional shallow water wave with concentrated interferences by the reflected waves, and could potentially alter the surface roughness as well.

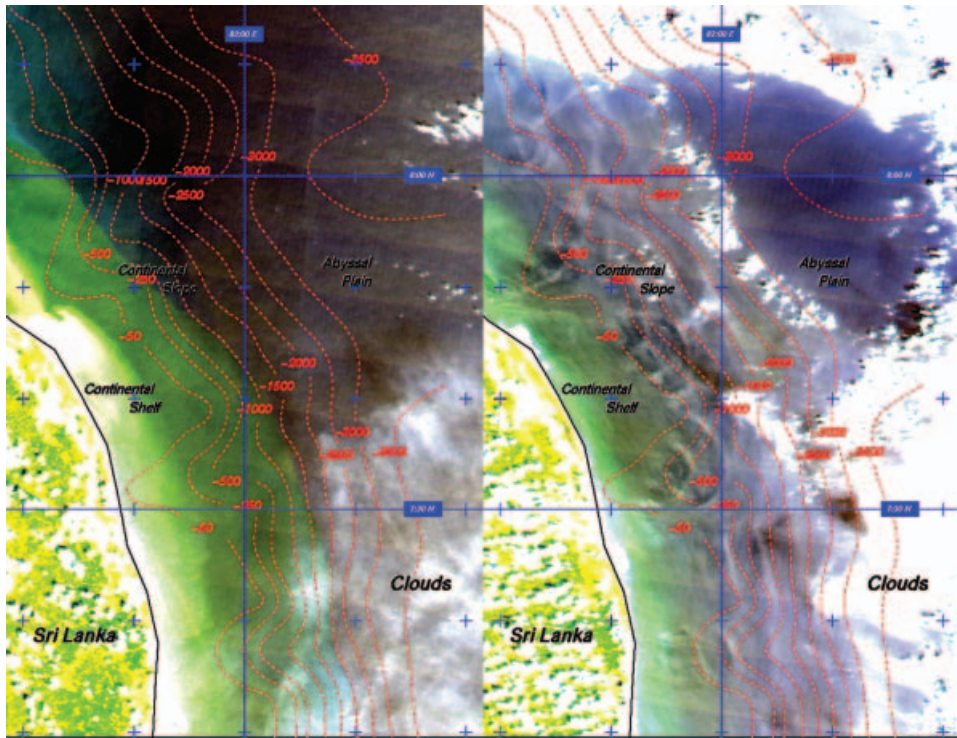


Figure 3. Reflected radiance of figure 2 overlaid with contours of the bathymetry data. The bathymetry data are from the National Geophysical Data Center (NGDC). We used the ETOPO2 global 2-min gridded elevation data interpolated and smoothed to match the higher resolution of the satellite data. The dashed contours are depths in metres.

In addition, the processes associated with particle transport and suspended material at the sea surface might be important to explain the MODIS images. Suspended matter in surface waters near the shelf break is related to biological processes, fluvial input from the shoreline, and upwelling of suspended sediment from the shelf and slope. There are two modes of sediment transport across the continental shelf (Cacchione and Drake 1990): (1) bed load, in which individual grains collide, roll or saltate in the thin bottom boundary layer; and (2) suspended load, in which the particles are advected with ambient currents. Increased particulate transport by strong shear currents in the bottom boundary layer and strong upward motion through the tsunami-induced wave enhances significantly the particle transport to the surface. The energetic internal waves are capable of modifying the bathymetric shape of the shelf and continental slope in a similar manner as has been reported by internal tides (Cacchione *et al.* 2002) and by storms (Nittrouer and Wright 1994).

Fascinatingly, the wave patterns appear in all MODIS visible channels (figure 4), indicating a detection of an altered surface either by a change in the surface roughness or suspended sediment or both. The waves are seen in the VNIR channels (figure 5(a)) even at a lower resolution, but they are not evident in the TIR channels (figure 5(c)). For the visible channels, suspended sediment is well correlated with the apparent upwelling radiance, but this correlation diminishes toward the

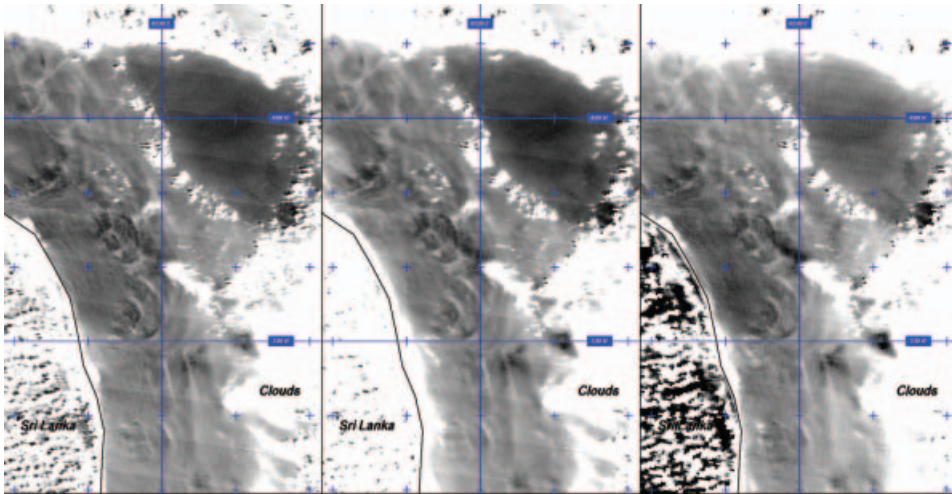


Figure 4. Reflected radiance of three MODIS bands that compose the three-colour image in figure 3. From left to right, they are band 1 (620–670 nm), band 4 (545–565 nm), band 3 (459–479 nm), corresponding to red, green, and blue, respectively.

near-infrared (wavelength 1000–3000 nm) (Curran and Novo 1988). Such a relationship has also been shown by Mobasher and Mousavi (2004) with a decrease in the correlation between suspended sediment and reflectance for the longer near-infrared wavelengths. Moreover, coarse material like sand found at the shelf of Sri Lanka is unlikely to stay resuspended for a long period of time (Kudraß pers. comm.). Because of this, the signal seen in the near-infrared channel (figure 5(b)) indicates that physical processes, like the interactions between internal

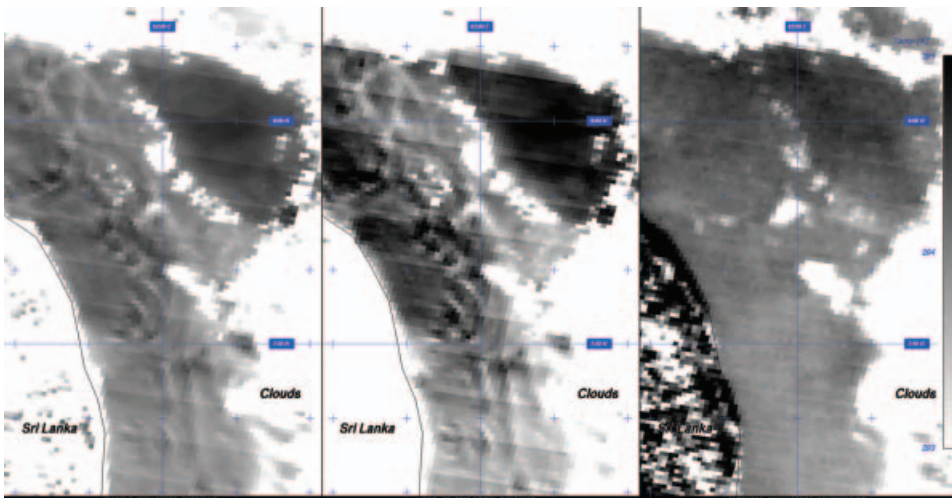


Figure 5. Left: reflected radiance of MODIS band 1 (620–670 nm, visible channel). Middle: reflected radiance of band 6 (1628–1652 nm, near infrared). Right: brightness temperature of band 31 (11000 nm, thermal infrared channel). These are 1-km data displayed at 250-m resolution.

wave-induced surface currents and surface waves, are detected. Significant alterations of the pycnocline and thermocline by internal waves may affect variations in the temperature near the sea surface (Farmer and Armi 1999). However, the brightness temperature in the TIR (figure 5(c)) does not support strong variations in the sea-surface temperatures.

In conclusion, the tsunami-induced wave patterns detected by MODIS are likely generated by internal waves, modified by interactions with surface waves, which result in changes in the surface roughness. It remains unclear, both theoretically and observationally, how these internal waves have substantially affected the suspended sediment concentration at the sea surface and how much these changes have affected the shelf break and continental slope. Thus, a clear understanding of vertical and horizontal mixing and its effect on the sediment transport is needed for future investigations.

An enhanced observational network including measurements of physical as well as biogeochemical parameters in regions of high tsunami frequency would be required to understand the complexity of the internal waves and wave interactions generated by a tsunami in detail. These data, together with remote-sensing data and a high-resolution bathymetry, could be assimilated into numerical models to investigate the wave pattern observed by satellite images. Such a test with existing models (e.g. Kowalik *et al.* 2005, Titov *et al.* 2005; NOAA Center for Tsunami Research; Farmer and Armi 1999) to explain these data will be a challenging and important task for the future and can contribute to an improved tsunami forecast by these models.

Acknowledgements

We thank Liam Gumley of the Space Science and Engineering Center, University of Wisconsin-Madison for providing figure 1. We also thank Klaus Hasselmann, Jim Gower, Herrman-Rudolf Kudraß, and Detlef Quadfasel for fruitful discussions improving the quality of the paper. A special acknowledgement goes to the reviewers of this paper, Dr Hui Fan and an anonymous reviewer, whose suggestions and comments were invaluable in improving the paper. Arne Winguth was supported by NASA grant NAG5-11245.

References

- BARNES, W.L., PAGANO, T.S. and SALOMONSON, V.V., 1998, Prelaunch characteristics of the Moderate Resolution Imaging Spectroradiometer (MODIS) on EOS-AM1. *IEEE Geoscience and Remote Sensing*, **36**, pp. 1088–1100.
- CACCHIONE, D.A. and DRAKE, C.A., 1990, Shelf sediment transport. In *The Sea, Vol. 9, Ocean Engineering Science*, B. LeMéhauté and D.M. Hanes (Eds), pp. 729–774 (New York: Wiley).
- CACCHIONE, D.A., PRATSON, L.F. and OGSTON, A.S., 2002, The shaping of continental slopes by internal tides. *Science*, **296**, pp. 724–727.
- CURRAN, P.J. and NOVO, E.M.M., 1988, The relationship between suspended sediment concentration and remotely sensed spectral radiance: a review. *Journal of Coastal Research*, **4**, pp. 351–368.
- CUTLER, A.N. and SWALLOW, J.C., 1984, Surface currents of the Indian Ocean (to 25° S, 100° E). In *IOS Technical Report 187*, 38 pp. (Wormely, UK: Institute of Oceanographic Sciences).
- DA SILVA J.C.B., ERMAKOV, S.A., ROBINSON, I.S., JEANS, D.R.G. and KIJASHKO, S.V., 1998, Role of surface films in ERS SAR signatures of internal waves on the shelf. 1. Short-period internal waves. *Journal of Geophysical Research*, **103**, pp. 8009–8031.

- EIGENHEER, A. and QUADFASEL, D., 1999, Seasonal variability of the Bay of Bengal circulation inferred from TOPEX/POSEIDON altimetry. *Journal of Geophysical Research*, **105**, pp. 3243–3252.
- FARMER, D. and ARMI, L., 1999, The generation and trapping of solitary waves over topography. *Science*, **283**, pp. 188–190.
- FARMER, D.R., 1978, Observations of long nonlinear waves in lakes. *Journal of Physical Oceanography*, **8**, p. 63.
- GARRET, C., 2003, Internal tides and ocean mixing. *Science*, **301**, pp. 1858–1859.
- GOWER, J., 2005, Jason 1 detects the 26 December 2004 tsunami. *EOS Transactions, AGU*, **86**, pp. 37–38.
- GUENTHER, B., GODDEN, G.D., XIONG, X., KNIGHT, E., QIU, S.-Y., MONTGOMERY, H., HOPKINS, M., KHAYAT, M. and HAO, Z., 1998, Prelaunch algorithm and data format for the Level 1 calibration products for the EOS-AM1 Moderate Resolution Imaging Spectroradiometer (MODIS). *IEEE Transactions on Geoscience and Remote Sensing*, **36**, pp. 1142–1151.
- HOTCHKISS, F.S. and WUNSCH, C., 1982, Internal waves in Hudson Canyon with possible geological implications. *Deep Sea Research*, **29**, pp. 415–442.
- INTERNATIONAL INDIAN OCEAN EXPEDITION, 1964, *International Indian Ocean Expedition USC&GS Ship Pioneer—1964. Volume 1. Cruise Narrative and Scientific Results* (Washington, DC: US Department of Commerce).
- KOWALIK, Z., KNIGHT, W., LOGAN, T. and WHITMORE, P., 2005, Numerical modelling of the global tsunami. *Science of Tsunami Hazard*, **23**, pp. 40–56.
- KUMAR, S. and RAMESH, R., 2005, Productivity measurements in the Bay of Bengal using the ¹⁵N tracer: Implications to the global carbon cycle. *Indian Journal of Marine Sciences*, **34**, pp. 153–162.
- LEBLOND, P.H. and MYSAK, L.A., 1978, *Waves in the Ocean* (Amsterdam: Elsevier).
- LIU, P.L.-F., LYNETT, P., FERNANDO, H., JAFFE, B.E., HIGMAN, B., MORTON, R., GOFF, J. and SYNOLAKIS, C., 2005, Observations by the International Tsunami Survey Team in Sri Lanka. *Science*, **308**, pp. 1595.
- MCCAVE, I.N., 2003, Sedimentary settings on continental margins—an overview. In *Ocean Margin Systems*, G. Wefer (Ed.), pp. 1–14 (Berlin: Springer).
- MOBASHERI, M.R. and MOUSAVI, H., 2004, Remote sensing of suspended sediments in surface waters using MODIS images. In *Proceedings of the XXth ISPRS Congress, Geo-Imagery Bridging Continent*, 12–23 July 2004, Istanbul, 140 pp.
- MOFJELD, H.O., TITOV, V.V., GONZALEZ, F.I. and NEWMAN, J.C., 2000, Analytic theory of tsunami wave scattering in the open ocean with application to the North Pacific Ocean. In *NOAA Technical Memorandum ERL PMEL-116*.
- NITTROUER, C.A. and WRIGHT, L.D., 1994, Transport of particles across continental shelves. *Reviews of Geophysics*, **32**, pp. 85–113.
- NOAA Center for Tsunami Research, 2005, Tsunami modeling and research. Available online at: <http://nctr.pmel.noaa.gov/model.html> (accessed 31 July 2005).
- OSBORNE, A.R. and BURCH, T.L., 1980, Internal solitons in the Andaman Sea. *Science*, **208**, pp. 451.
- PENNISH, E., 2005, Powerful tsunami's impact on coral reefs was hit and miss. *Science*, **307**, pp. 657.
- PETTY, G.W., 2004, *A First Course in Atmospheric Radiation*, pp. 110–145 (Madison, WI: Sundog).
- QUADFASEL, D., 1998, RV SONNE 126/127 cruise Bay of Bengal and Arabian Sea BENGALWOCE. Available online at: http://www.ifm.uni-hamburg.de/~wwwro/WOCE/web_sonne/sonne_fb.html (accessed 31 July 2005).
- SMALL, J., 2001a, A nonlinear model of the shoaling and refraction of interfacial solitary waves in the ocean. Part I: Development of the model and investigation of the shoaling effect. *Journal of Physical Oceanography*, **31**, pp. 3163–3183.

- SMALL, J., 2001b, A nonlinear model of the shoaling and refraction of interfacial solitary waves in the ocean. Part II: Oblique refraction across a continental slope and propagation over a seamount. *Journal of Physical Oceanography*, **31**, pp. 3184–3199.
- SRINIVAS, K., DINESH KUMAR, P.K. and REVICHANDRAN, C., 2005, ENSO signature in the sea level along the coastline of the Indian subcontinent. *Indian Journal of Marine Sciences*, **34**, pp. 225–236.
- TAKAYAMA, K. and SAITO, T., 2004, Shock wave/geophysical and medical applications. *Annual Review of Fluid Mechanics*, **36**, pp. 347–379.
- TITOV, V., RABINOVICH, A.B., MOJFELD, H.O., THOMSON, R.E. and GONZALES, F.I., 2005, The Global Reach of the 26 December 2004 Sumatra Tsunami. *Science*, **309**, pp. 2045–2048.
- TORO, E.F., OLIM, M. and TAKAYAMA, K., 1999, Unusual increase in tsunami wave amplitude at the Okushiri Island: Mach reflection of shallow water waves. In *Proceedings of the 22nd International Symposium on Shock Waves*, **2**, G. J. Ball, R. Hillier and G. T. Roberts (Eds.), pp. 1207–1212.
- WYRTKI, K., 1973, Physical oceanography of the Indian Ocean. In *The Biology of the Indian Ocean*, B. Zeitzschel (Ed.), pp. 18–36 (Berlin: Springer).